Luminescent dinuclear copper(I) halide complexes double bridged by diphosphine ligands: Synthesis, structure characterization, properties and TD-DFT calculations

ARTICLE *in* POLYHEDRON · OCTOBER 2014

Impact Factor: 2.01 · DOI: 10.1016/j.poly.2014.07.034

11 AUTHORS, INCLUDING:

Kangying Shu
China Jiliang University
51 PUBLICATIONS **248** CITATIONS
SEE PROFILE

Wenxiang Chai
China Jiliang University
50 PUBLICATIONS **150** CITATIONS
SEE PROFILE

Polyhedron 81 (2014) 687–694

Contents lists available at ScienceDirect

Polyhedron

journal homepage: www.elsevier.com/locate/poly

Luminescent dinuclear copper(I) halide complexes double bridged by diphosphine ligands: Synthesis, structure characterization, properties and TD-DFT calculations

Xiayi Zhang [a], Li Song [b], Mingwei Hong [a], Hongsheng Shi [a], Kaijie Xu [a], Qizhong Lin [a], Yi Zhao [a], Yuan Tian [a], Jiafeng Sun [a], Kangying Shu [a], Wenxiang Chai [a,c,*]

[a] College of Materials Science and Engineering, China Jiliang University, Hangzhou 310018, PR China
[b] Key Laboratory of Advanced Textile Materials and Manufacturing Technology of Education Ministry, Department of Chemistry, Zhejiang Sci-Tech University, Hangzhou 310018, PR China
[c] State Key Laboratory of Structural Chemistry, Fujian Institute of Research on the Structure of Matter, Chinese Academy of Sciences, Fuzhou 350002, PR China

ARTICLE INFO

Article history:
Received 3 May 2014
Accepted 13 July 2014
Available online 1 August 2014

Keywords:
Luminescence
Copper(I) halide complex
Diphosphine ligand
X-ray crystal structure
(TD-)DFT calculation

ABSTRACT

Four luminescent copper(I) halide complexes of the type $[CuXPh_2P(CH_2)_nPPh_2]$ [X = I, n = 4 (**1**), 5 (**2**); X = Br, n = 4 (**3**), 5 (**4**)] were prepared by reacting CuX with the appropriate diphosphine in a 1:1 M ratio. All the complexes were characterized by spectroscopic analysis (IR, UV–Vis), elemental analysis and photoluminescence studies. Single-crystal X-ray diffraction revealed that **1** and **2** are both dinuclear structures which are constructed by two μ-I bridges and, especially, two diphosphine ligands as μ_2 bridges. The copper(I) iodide complexes are thermally stable, and **2** melts at 242 °C. All the complexes exhibit a strong emission in the solid state. The excited states have been assigned as a halide-to-ligand charge transfer (XLCT) state mixed with a small amount of a metal-to-ligand charge transfer (MLCT) transition, based on the TD-DFT calculations. The calculated electronic transitions have also been compared with the experimental absorption spectra to understand the reason why there is some blue-shift of the low-energy band when the halide atom changes from iodine to bromine, and an even greater blue-shift when the ligand changes from DPPP to DPPB.

1. Introduction

Highly luminescent transition metal complexes are widely studied due to their broad applications in organic electroluminescence (OEL) [1], solar energy conversion [2], light-driven fuel production [3,4], photochemical catalysis [5], luminescence-based sensors [6] and probes of biological systems [7]. Each of these applications imposes specific demands on the materials, such as chemical or electrochemical stability, color and color purity of the emitted light, high emission quantum yield, specific emission decay time and so on [8]. For instance, cyclometallated d^6 and d^8 complexes of the third row transition series, especially iridium(III), have been employed in OEL products because of their high phosphorescence quantum yield, wavelength tenability and thermal stability [9]. However, the use of these materials inevitably involves other inherent questions, such as high cost, limited availability and toxicity of the precious metals [10]. In view of these disadvantages, there is considerable interest in developing luminescent complexes of the abundant, cheap and non-toxic metal, copper [11].

Previously, there have been numerous studies on copper(I) complexes, focusing on either their structural chemistry or their luminescence. The first important system is $[Cu(NN)_2]^{1+}$ complexes which present luminescence that is markedly dependent on the nature of the ligands. Some systematic studies have reported that the luminescence originates from an MLCT excited state, and the major non-radiative decay for the MLCT state is related to two structural distortions of flattening and rocking due to the Jahn–Teller effect of copper(II) [7,12]. In order to inhibit these distortions, bulky substituents have been introduced into the phenanthroline ligand at the 2,9-positions, and this method has been proved to be useful in improving the luminescent quantum yield. Similarly, the heteroleptic $[Cu(NN)P_2]^{1+}$ complexes with sterically crowded ligands, such as $[Cu(dbp)(POP)]^{1+}$, also show a high luminescent yield [13]. The other one important structure is tetranuclear cube-like copper(I) halide clusters, $[CuXL]_4$ (X = halogen, L = pyridine or phosphine ligand), which shows not only strong

* Corresponding author at: College of Materials Science and Engineering, China Jiliang University, Hangzhou 310018, PR China. Tel.: +86 0571 86835738.
E-mail address: wxchai@cjlu.edu.cn (W. Chai).

http://dx.doi.org/10.1016/j.poly.2014.07.034
0277-5387/

emission in both the solid or solution states at room temperature but also fascinating thermochromic luminescence behavior [14,15]. Theoretic studies on two different emission bands of these complexes revealed that the low energy phosphorescence is attributed to a cluster-centered (^{3}CC) state and the other to a halogen to ligand charge transfer (^{3}XLCT) state.

Recently, Bräse et al. reported that dinuclear halogen-bridged copper(I) complexes based on diphenylphosphinopyridine-type P^N ligands show a very high luminescence quantum yield in the solid state [16,17]. These highly emissive materials have been regarded as an attractive singlet-harvesting emitter which benefit from a thermally activated delayed fluorescence (TADF) approach, based on a small energy gap between the S_1 and T_1 states [8]. However, there is still a scarcity of good candidates with high luminescent efficiency for various applications, and rarity of the corresponding theoretic calculations, especially on the emerging molecules of dinuclear halogen-bridged copper(I) complexes. In the present paper, we have studied the absorption and emission of four dinuclear halogen-bridged copper(I) complexes constructed from the diphosphine ligands DPPB and DPPP. Theoretical studies based on (TD-)DFT calculations also been carried out on these complexes to understand their luminescent properties.

2. Experimental

2.1. Materials and general methods

All the reagents were purchased commercially and employed without further purification. Infrared spectra were measured with a Bruker Tensor27 FT-IR spectrophotometer in the range 4000–400 cm^{-1} in KBr lamella. The UV–Vis and fluorescence spectral measurements were performed on Shimadzu UV3600 and Horiba Jobin–Yvon FL3–211-P spectrometers at room temperature, respectively. TGA-DSC curves were obtained in a static high purity argon atmosphere with a Mettler Toledo Simultaneous Thermal Analyzer at a heating rate of 10 °C/min.

2.2. Synthesis

2.2.1. [$CuIPh_2P(CH_2)_4PPh_2$] (**1**)

A solution of cuprous iodide (0.019 g, 0.1 mmol) in CH_3CN (5 mL) was mixed with a solution of 1,4-bis(diphenylphosphino)butane (DPPB) (0.043 g, 0.1 mmol) in CH_2Cl_2 (5 mL) to produce a white precipitate in 82% yield. Colorless crystals for the diffraction study were obtained from the mother solution by slow

Table 1
Crystal data and structure refinement for **1** and **2**.

Parameter	Compound	
	1	**2**
Empirical formula	$C_{56}H_{56}Cu_2I_2P_4$	$C_{58}H_{60}Cu_2I_2P_4$
Color and habit	colorless block	colorless block
Crystal size (mm)	0.20 × 0.13 × 0.11	0.20 × 0.13 × 0.12
Crystal system	triclinic	triclinic
Space group	$P\bar{1}$	$P\bar{1}$
a (Å)	10.2805(6)	9.9143(7)
b (Å)	11.2895(6)	11.7428(6)
c (Å)	12.1393(6)	12.2391(6)
α (°)	70.073(5)	104.439(4)
β (°)	86.801(4)	97.588(5)
γ (°)	78.032(5)	94.680(5)
V (Å^3)	1295.59(12)	1358.04(14)
Z	1	1
Formula weight	1233.79	1261.82
$D_{cal.}$ (Mg/m^3)	1.581	1.543
Absorption coefficient (mm^{-1})	2.172	2.074
F(000)	616	632
Parameter/restraints/data (obs.)	289/0/3794	298/0/4024
Final R indices (obs.)	R_1 = 0.0372, wR_2 = 0.0568	R_1 = 0.0352, wR_2 = 0.0585
R indices (all)	R_1 = 0.0564, wR_2 = 0.0641	R_1 = 0.0521, wR_2 = 0.0643
Goodness-of-fit (GOF)	1.002	0.980
Largest and mean delta/sigma	0.001, 0.000	0.000, 0.000
Largest difference peak (e Å^{-3})	0.510, −0.505	0.478, −0.504

Table 2
Selected bond lengths (Å) and angles (°) for **1** and **2** from X-ray experiments and DFT calculations.

	Exp.	Cal.		Exp.	Cal.
*Compound **1***					
Cu(1)–P(1)	2.2711(12)	2.3900	Cu(1)–P(2)	2.2798(10)	2.3981
Cu(1)–I(1)	2.7438(5)	2.8310	Cu(1)–I(1)^{i}	2.7307(5)	2.8029
I(1)–Cu(1)^{i}	2.7307(5)	2.8029			
P(1)–Cu(1)–P(2)	124.50(4)	124.609	P(1)–Cu(1)–I(1)^{i}	116.51(3)	113.872
P(2)–Cu(1)–I(1)^{i}	98.46(3)	98.440	P(1)–Cu(1)–I(1)	99.77(3)	101.150
P(2)–Cu(1)–I(1)	107.93(3)	108.318	I(1)–Cu(1)–I(1)^{i}	109.215(19)	110.303
*Compound **2***					
Cu(1)–P(1)	2.2623(10)	2.3945	Cu(1)–P(2)	2.2589(11)	2.3931
Cu(1)–I(1)	2.7486(5)	2.8124	Cu(1)–I(1)^{ii}	2.7078(5)	2.8049
I(1)–Cu(1)^{ii}	2.7078(5)	2.8049			
P(2)–Cu(1)–P(1)	121.01(4)	121.150	P(2)–Cu(1)–I(1)^{ii}	115.42(3)	114.808
P(1)–Cu(1)–I(1)^{ii}	104.47(3)	103.759	P(2)–Cu(1)–I(1)	103.63(3)	102.749
P(1)–Cu(1)–I(1)	114.04(3)	113.351	I(1)^{ii}–Cu(1)–I(1)	95.632(15)	99.119

Symmetry code: (i) $-x+1, -y, -z+1$; (ii) $-x, -y+1, -z$.

Table 3
Some strong low-energy singlet electronic transitions for **1**–**4** calculated by TD-DFT.

Complex	Transition	Energy (10^3 cm^{-1})	Wavelength (nm)	Oscillator strength	Major contributions
1	S_1	30.9	323.3	0.0221	HOMO → LUMO (93%) H−1 → LUMO (2%)
	S_4	31.6	316.0	0.0135	HOMO → L+3 (+83%) H−1 → LUMO (9%) H−3 → L+2 (+4%)
	S_5	31.7	315.7	0.0054	H−1 → LUMO (+82%) HOMO → L+3 (+9%) HOMO → LUMO (+3%) H-4 → L+1 (+3%)
	S_8	33.1	302.4	0.0322	HOMO → L+4 (+60%) H-1 → L+3 (31%) HOMO → L+6 (3%)
	S_9	33.1	302.2	0.0521	H−1 → L+3 (+56%) HOMO → L+4 (+35%) HOMO→L+3 (2%)
2	S_1	30.7	326.0	0.0032	HOMO → LUMO (+91%) H-4 → L+1 (+4%) H-1 → L+3 (+2%)
	S_3	30.9	323.6	0.0447	H−1 → LUMO (+58%) HOMO → L+3 (+36%) H-4 → L + 2 (+3%)
	S_5	31.2	320.2	0.0030	HOMO → L+3 (+57%) H−1 → LUMO (38%)
	S_8	31.8	314.4	0.0095	H−2 → LUMO (+91%) H−1 → L+3 (+4%)
	S_9	32.1	312.0	0.0073	H−1 → L+3 (+89%) H−2 → LUMO(5%)HOMO− > LUMO(2%)
3	S_1	31.5	317.9	0.0322	HOMO → LUMO(+88%) H−1 → LUMO(+3%) HOMO → L+3 (2%) H−4 → L+1 (2%)
	S_4	31.9	313.3	0.0044	HOMO → L + 3 (+44%) H−1 → LUMO (+44%) H−2 → L+2 (4%) H−4 → L+1 (3%) H−2 → L+1 (2%)
	S_5	32.4	308.7	0.0107	H−1 → LUMO (+42%) HOMO → L + 3 (41%) HOMO → LUMO (7%) H-2 → L+1(3%) H−1 → L+3(+2%)
	S_8	33.2	301.5	0.0063	H−1 → L+3 (+82%) HOMO → L+3 (+6%) H-2 → L+2 (+6%)
	S_9	33.6	297.7	0.0570	HOMO → L + 4 (+95%)
4	S_1	30.8	324.7	0.0157	HOMO → LUMO (+90%) H−3 → L+1 (7%)
	S_4	31.3	319.8	0.0102	HOMO → L+3 (+85%) H-3 → L+2 (+10%) H-1 → LUMO (+4%)
	S_5	32.6	307.0	0.0199	H−1 → LUMO (+91%) HOMO → L+3 (4%)
	S_8	32.9	303.7	0.0072	H−2 → LUMO (+92%) HOMO → L+4 (+2%)
	S_9	33.0	302.7	0.0027	H−1 → L+3 (+74%) HOMO → L+4(+15%) H−2 → LUMO (3%)

evaporation of the solvent over about a week. IR (cm^{-1}): 3050(w), 2902(w), 2844(w), 1586(w), 1486(m), 1437(s), 1097(m), 740(s), 692(vs), 513(s), 482(m). *Anal.* Calc. for $C_{56}H_{56}Cu_2I_2P_4$: C, 54.51; H, 4.57. Found: C, 54.11; H, 4.04%.

2.2.2. $[CuIPh_2P(CH_2)_5PPh_2]$ (**2**)

A solution of cuprous iodide (0.019 g, 0.1 mmol) in CH_3CN (5 mL) was mixed with a solution of 1,5-bis(diphenylphosphino)pentane (DPPP) (0.044 g, 0.1 mmol) in CH_2Cl_2 (5 mL) to produce a colorless solution. After stirring for an hour, the solvents were removed under reduced pressure to give a white residue which was then washed with CH_3CN and EtO, and dried in air. Yield: 97%. Crystals for the diffraction study were obtained from same solution by slow evaporation of the solvent over about a week. M.p. 242 °C. IR (cm^{-1}): 3047(w), 2922(w), 2858(w), 1584(w), 1480(m), 1432(s), 1098(m), 744(s), 697(vs), 506(s). *Anal.* Calc. for $C_{58}H_{60}Cu_2I_2P_4$: C, 55.20; H, 4.79. Found: C, 55.76; H, 4.21%.

2.2.3. $[CuBrPh_2P(CH_2)_4PPh_2]$ (**3**)

Complex **3** was prepared following a similar procedure to that for **1**, only using cuprous bromide instead of cuprous iodide. Yield: 79%. IR (cm^{-1}): 3051(w), 2897(w), 2851(w), 1584(w), 1484(m), 1437(s), 1101(m), 735(s), 691(vs), 516(s), 481(m). *Anal.* Calc. for $C_{56}H_{56}Cu_2Br_2P_4$: C, 59.01; H, 4.95. Found: C, 59.55; H, 4.63%.

2.2.4. $[CuBrPh_2P(CH_2)_5PPh_2]$ (**4**)

Complex **4** was prepared following a similar procedure to that for **2**, only using cuprous bromide instead of cuprous iodide. Yield:

92%. IR (cm^{-1}): 3049(w), 2897(w), 2858(w), 1585(w), 1484(m), 1434(s), 1100(m), 740(s), 697(vs), 510(s). *Anal.* Calc. for $C_{58}H_{60}Cu_2Br_2P_4$: C, 59.65; H, 5.18. Found: C, 59.06; H, 5.71%.

2.3. Crystal structure determination

Diffraction intensities for complexes **1** and **2** were collected at 20 °C on an Oxford Xcalibur (Atlas Gemini ultra) diffractometer with the ω-scan technique (see Table 1). The structures were solved with the direct method and refined with full-matrix least-squares using the SHELX package [18,19]. Anisotropic displacement parameters were applied to all non-hydrogen atoms, and the organic hydrogen atoms were generated geometrically (C–H 0.96 Å). Selected bond lengths and angle parameters are collected in Table 2 for the two complexes.

2.4. Theoretical calculations

The calculations described here were carried out using the Gaussian 09 suite of programs [20]. The structures of the four Cu(I) iodide/bromine complexes were fully optimized in the ground state (S_0) using the DFT method with the three-parameters hybrid functional B3LYP and the LACVP* basis set [21,22], which is a combination basis set including the relativistic effective core potential standard basis set LANL2DZ for Cu, P and I/Br and the standard 6-31G* basis set for C and H. Polarization functions were also added for P and I/Br, i.e. P (ξ(d) = 0.34) and I (ξ(d) = 0.266)/Br(ξ(d) = 0.389) [23]. The optimized molecular structure parameters in the S_0 states are summarized in Table 2 for **1** and **2**. To obtain estimates of the vertical electron excitation energies, which include some account of the electron correlation, time-dependent density functional theory (TD-DFT) was performed on the calculated S_0 geometries using same B3LYP method and LACVP* basis set. The excitation energies, oscillator strength parameters and corresponding major orbital contributions for the five main electronic transitions are gathered in Table 3 for the four complexes.

3. Results and discussion

3.1. Structural characterization

The X-ray diffraction data revealed that complex **1** has an isolated dinuclear structure with a four-membered $\{Cu_2(\mu_2\text{-}I)_2\}$ ring, in which each Cu(I) atom exhibits a tetrahedral configuration constructed by two μ_2-I and two P atoms from two μ_2-bridged DPPB ligands. The $\{Cu_2I_2\}$ unit is planar, as is usual for halogen-bridged copper complexes, and its midpoint coincides with the crystallographic inversion center of the molecule. On the two sides of the $\{Cu_2I_2\}$ plane, as shown in Fig. 1, two DPPB ligands bridge the two Cu atoms, so that the dinuclear structure is supported further. To date, many similar double bridged structures supported by DPPM ligand, due to its suitable linkage distance, have been reported [24–27], however, these double bridged structures in cuprous coordination chemistry are very rare when the DPPM ligand is replaced by the other diphosphine ligands [28–30]. The two Cu–I bond lengths of 2.7307(5) and 2.7438(5) Å are similar to those previously reported [31]. The two Cu–P bond lengths of 2.2711(12) and 2.2798(10) Å and the P–Cu–P angle of 124.50(4)° are all comparable to those of reported copper-phosphine complexes [11]. No obvious intra-molecular π–π stacking interactions could be found between any two aromatic rings. In the solid state, the molecules of **1** are only stabilized by weak Van der Waals' forces, without any obvious hydrogen bonding or π–π stacking interactions (Fig. 2).

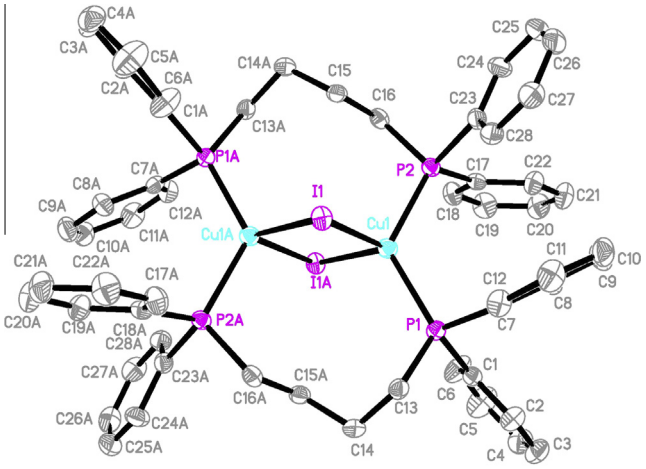

Fig. 1. The isolated dinuclear molecular structure of complex **1**.

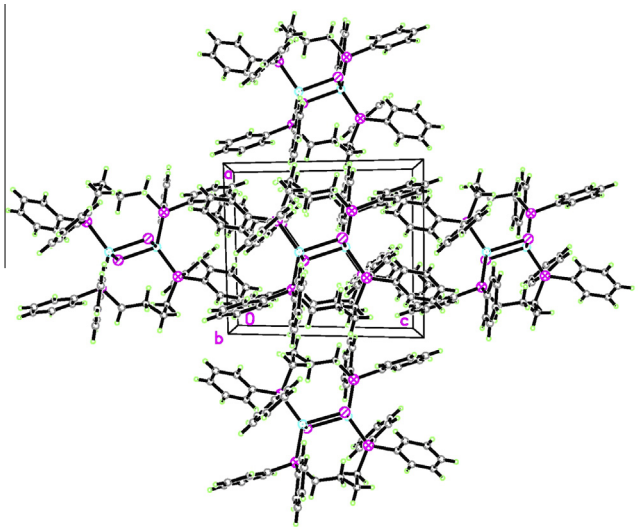

Fig. 2. The packing diagram of complex **1**.

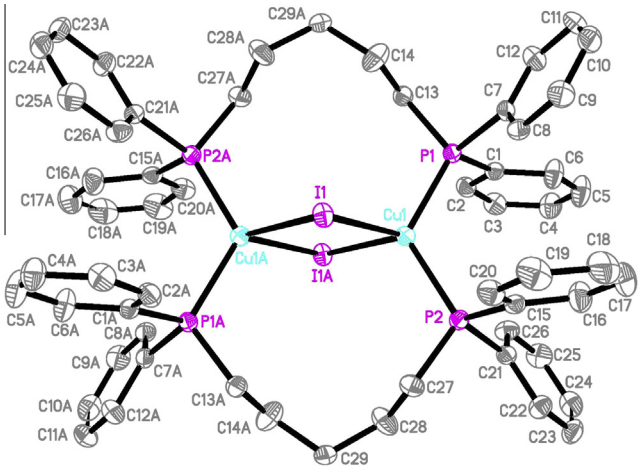

Fig. 3. The isolated dinuclear molecular structure of complex **2**.

As shown in Fig. 3, similar to **1**, complex **2** is still an isolated dinuclear structure, except that the μ_2-bridging ligand is DPPP instead of DPPB. The Cu(I) atom exhibits a tetrahedral configuration, coordinated by two μ_2-I and two P atoms from two

μ_2-bridged DPPP ligands. In its core $\{Cu_2I_2\}$ unit, the two Cu–I bond lengths of 2.7078(5) and 2.7486(5) are still within the range of reported lengths [31], but they are more different from each other than observed in **1**. Moreover, the Cu–P bond lengths of 2.2589(11) and 2.2623(10) Å and the P–Cu–P angle of 121.01(4)° are all smaller than that in **1**. All of these changes should be the result of the ligand swapping from DPPB to DPPP; in detail, the longer alkyl linker of DPPP not only shortens the Cu–P bond length due to its stronger electron donating ability, but it also compresses the two Cu–P bonds, leading to a smaller P–Cu–P angle due to the bigger size of the $-(CH_2)_5-$ linker. This bigger linker also lengthens the Cu—Cu distance (3.371 Å in **1** *versus* 3.664 Å in **2**) so that the $\{Cu_2I_2\}$ unit is more loose in **2** and the Cu–I bond lengths are more different from each other in **2**. In the solid state, the molecules of **2** are also only stabilized by weak Van der Waals' forces, without any obvious intra- or inter-molecular hydrogen bonding or π-π stacking interactions (Fig. 4).

Based on the crystallographic data, the calculated molecular structures of **1** and **2** in the gas phase have also been studied at the B3LYP level, without any geometric restrains. Obviously, as reported in the literature [32], all of the bond lengths herein are overestimated compare to the experimental data (Table 2), but all the differentiations of the two molecules are still visible from the calculated data and are in reasonable agreement with the crystallographic data, including the previously mentioned bond lengths and angles. Accordingly, the aforementioned linker effect on the molecular structure could also be supported by the DFT calculations. In addition, the calculated IR spectra are both coincident with the experimental spectra (see Fig. S1).

3.2. TG–DSC analysis

The coinstantaneous TG and DSC curves obtained on the polycrystalline samples of **1** and **2** are shown in Fig. 5, where the purities of the samples have first been checked by PXRD measurements. The TG and DSC curves show that **1** is stable ranging from room temperature to 285 °C. The complex then has a great weight loss of 72.65% from 285 to 450 °C and a slow weight loss after 450 °C. Finally, there is almost no residuum, probably due to the fact that the decomposition product is volatile. As shown in Fig. 5b, the DSC curve shows that there is an endothermic peak at about 240 °C for **2** in its TG plot, however there is no obvious sign of decomposition. Further measurement of the melting point indicated that **2** begins to melt from 242 °C. After melting, the TG curve proves that **2** is stable up to 310 °C, then the complex has a great weight loss of 72.09% from 310 to 460 °C, and a slow weight loss after 460 °C. The residuum of **2** should be inorganic compound with 5.43% at about 800 °C. In general, the thermal stability of this material is good; its melting temperature of 242 °C is especially very suitable for using non-solution processes to fabricate devices, e.g. OLEDs [33].

3.3. UV absorption spectra

The electronic absorption spectra of complexes **1**–**4**, recorded on the as-synthesized powder samples, are shown in Fig. 6. There are two different bands in their absorption spectra in the range 200–400 nm: one broad band observed at 200–300 nm and the other stronger band observed at 300–400 nm. In the high energy

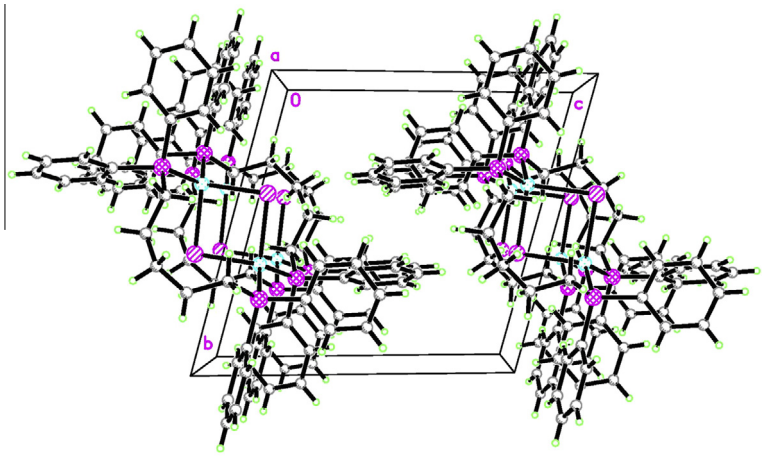

Fig. 4. The packing diagram of complex **2**.

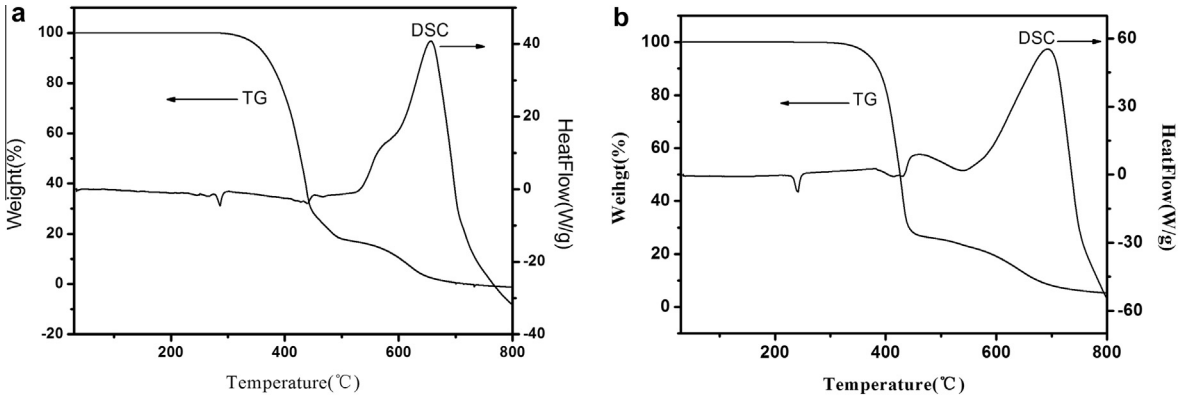

Fig. 5. The TG and DSC curves of: (a) complex **1** and (b) complex **2**.

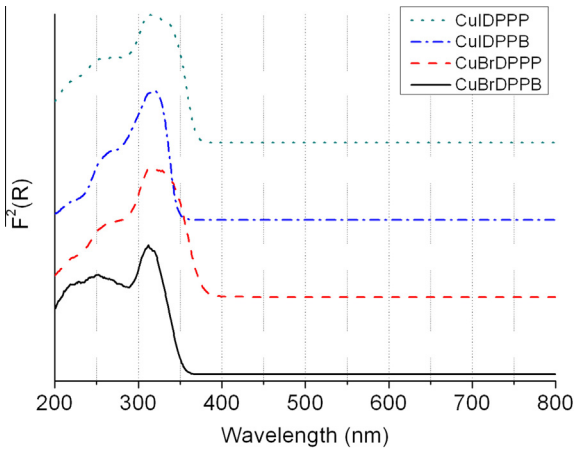

Fig. 6. The UV absorption spectra of complex **1**–**4** in the solid state.

region, the ligand-centered (π–π^*) transition of the diphosphine ligands should be dominant [34]. The low-energy transition should be derived from a charge transfer mechanism, which should be either assigned as a metal to ligand charge transfer (MLCT) or as a halide to ligand charge transfer (XLCT), according to previous literature [11]. These assignments were further investigated and identified by theoretical calculations on complexes **1**–**4** using time-dependent density functional theory (TD-DFT). The frontier orbitals for these compounds are shown in Fig. 7, and other molecular orbitals related to the lowest energy transition states (Table 3) are also shown in Figs. S2–S5. In each complex, the HOMO is largely localized on the Cu_2X_2 core, with minor participation of the phosphorus atom of the diphosphine ligand. Furthermore, it is comprised primarily of μ_2-X non-bond p orbitals mixed with varying degrees of Cu–d character. On the other hand, the LUMO is entirely located on the diphosphine ligand, and is mainly delocalized over the π^* orbitals of the phenyl groups. Actually, as shown in Table 3 and Figs. S2–S5, five strong low-energy absorptions in each complex were all found to be transitions from the Cu_2X_2 core to the diphosphine ligand, with the characters of each excited state being similar to the HOMO → LUMO excited state (S_1 state) in complex **1**. Therefore, it is certain that the low-energy band observed in experimental absorption spectra should be mainly assigned as XLCT mixed with a little MLCT transition. The calculated electronic absorption spectra that focus on 10 low-energy transition singlet states for complexes **1**–**4** are also shown in Fig. 8. In accordance with the experimental spectra, there is some blue-shift of the low-energy band when the halide atom changes from iodine to bromine, and an even greater blue-shift when the ligand changes from DPPP to DPPB. The effect of altering the halide should result from the decrease in polarizability on going from iodine to bromine, or the decrease of their delocalization [35]. The later effect of the ligand should be attributed to the stronger donation of the $-(CH_2)_5-$ linker in DPPP because the donating group could decrease the HOMO–LUMO gap, leading to a smaller excited energy [36].

3.4. Luminescence properties

Previously, the luminescent properties of copper(I) halide complexes have been studied not only focusing on the synthetic chemistry but also the structural chemistry [11,34]. In 1999, Ford P.C. reviewed the photoluminescence (PL) properties of many multinuclear copper(I) compounds and summarized five possible excited states for luminescent mechanisms, typically MLCT, XLCT, halide to metal charge transfer (XMCT), metal-centered (MC) and cluster

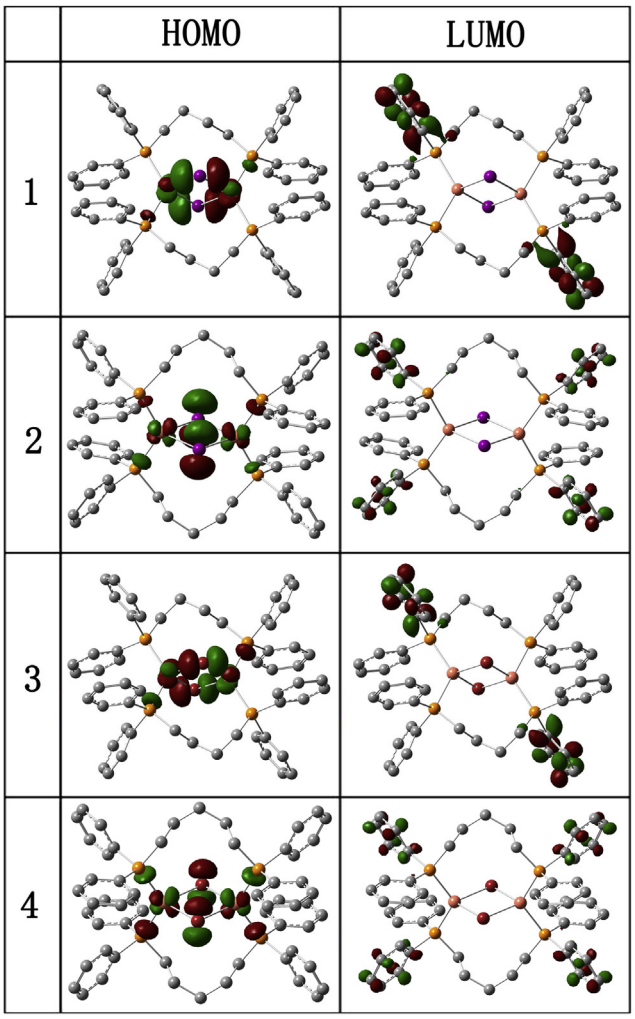

Fig. 7. HOMO and LUMO frontier orbital plots of complexes **1**–**4** based on TD-DFT calculations.

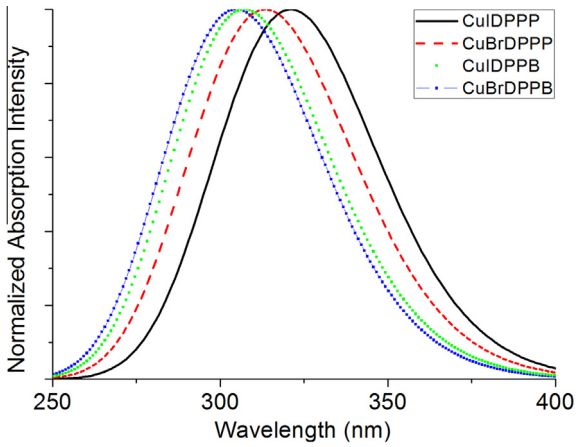

Fig. 8. The calculated electronic absorption spectra of complexes **1**–**4** focused on the 10 lowest energy transitions.

centered (CC) excited states [14]. In this case, the light emitting from the powder sample is strong for each complex at room temperature. As shown in Fig. 9, although the band shapes in the PL excitation spectra of complexes **1**–**4** do not agreed with the corresponding UV absorption spectra, similar shifts are also observed

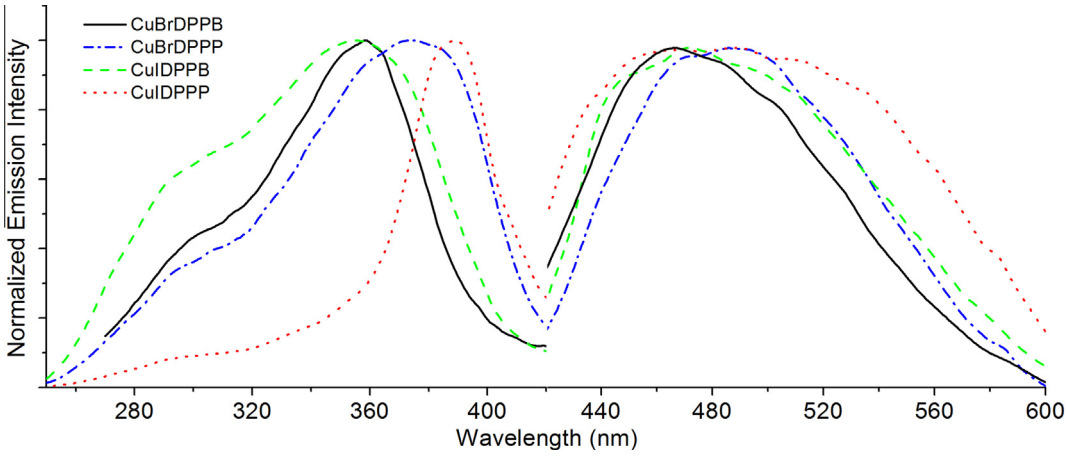

Fig. 9. The PL excitation and emission spectra of complexes **1**–**4** as a powder samples.

herein. The PL excitations could then also be assigned as (XLCT + MLCT), just like the absorption spectra. Different from the excitation spectra, the PL emission spectra appear to be more complicated, which could be the result of many photophysical processes or structural relaxations of these complexes. For example, the PL emission band of complex **2** is broader than the others, presumably the reason for this is that the molecular structure of **2** is loosest and the DPPP ligand is more flexible, so that its structural relaxation is more severe. Consequently, the PL emission intensity of complex **2** is also weaker than the others. Thus for a high efficiency of the PL emission, it is not good to employ diphosphine ligands with a long flexible linker, although it could reduce the excited energy.

4. Conclusion

A series of luminescent complexes, $[CuXPh_2P(CH_2)_nPPh_2]$ [X = I, n = 4 (**1**), 5 (**2**); X = Br, n = 4 (**3**), 5 (**4**)], have been synthesized and characterized. X-ray diffraction studies determined that **1** and **2** are both dinuclear structures with a Cu_2I_2 core, which is formed by two μ-I bridges and further supported by two μ_2 diphosphine ligands. All the complexes exhibit a strong CT absorption band which has been assigned as XLCT mixed a little MLCT transition, as confirmed by TD-DFT calculations. When the X atom changes from iodine to bromine, or the ligand changes from DPPP to DPPB, some blue-shift of the CT band has been observed, both in the experimental absorption spectra as well as in the calculated ones. These two types of blue-shifts should be the result of a decrease in the polarizability on going from iodine to bromine, and the stronger electron donation of the $-(CH_2)_5-$ linker in DPPP. These complexes show intense room temperature luminescence in the solid state, most likely originating from emissive excited states of major XLCT and a little MLCT character, according to the excitation spectra and TD-DFT calculations. Thermal analyses on the copper(I) iodide complexes showed them to be suitable for fabricating luminescent devices because of their good thermal stability.

Acknowledgments

The authors are grateful for financial support from the National Natural Science Foundation of China (Project Nos. 61205184 and 11175169), the Foundation of State Key Laboratory of Structural Chemistry (project no. 20110011), and the Natural Science Foundation of Zhejiang Province (Project No. LY12E02010).

Appendix A. Supplementary data

CCDC 990122 and 990123 contains the supplementary crystallographic data for **1** and **2**. These data can be obtained free of charge via http://www.ccdc.cam.ac.uk/conts/retrieving.html, or from the Cambridge Crystallographic Data Centre, 12 Union Road, Cambridge CB2 1EZ, UK; fax: (+44) 1223-336-033; or e-mail: deposit@ccdc.cam.ac.uk. Supplementary data associated with this article can be found, in the online version, at http://dx.doi.org/10.1016/j.poly.2014.07.034.

References

[1] R.D. Costa, E. Ortí, H.J. Bolink, F. Monti, G. Accorsi, N. Armaroli, Angew. Chem., Int. Ed. 51 (2012) 8178.
[2] N. Robertson, ChemSusChem 1 (2008) 977.
[3] T. Stoll, M. Gennari, J. Fortage, C.E. Castillo, M. Rebarz, M. Sliwa, O. Poizat, F. Odobel, A. Deronzier, M.-N. Collomb, Angew. Chem., Int. Ed. 126 (2014) 1680.
[4] S.-P. Luo, E. Mejía, A. Friedrich, A. Pazidis, H. Junge, A.-E. Surkus, R. Jackstell, S. Denurra, S. Gladiali, S. Lochbrunner, M. Beller, Angew. Chem., Int. Ed. 52 (2013) 419.
[5] Y. Kuramochi, M. Kamiya, H. Ishida, Inorg. Chem. 53 (2014) 3326.
[6] Q.A. Zhao, F.Y. Li, C.H. Huang, Chem. Soc. Rev. 39 (2010) 3007.
[7] D.R. McMillin, K.M. McNett, Chem. Rev. 98 (1998) 1201.
[8] R. Czerwieniec, J. Yu, H. Yersin, Inorg. Chem. 50 (2011) 8293.
[9] L. Xiao, Z. Chen, B. Qu, J. Luo, S. Kong, Q. Gong, J. Kido, Adv. Mater. 23 (2011) 926.
[10] O. Green, B.A. Gandhi, J.N. Burstyn, Inorg. Chem. 48 (2009) 5704.
[11] N. Armaroli, G. Accorsi, F. Cardinali, A. Listorti, Photochemistry and photophysics of coordination compounds: copper, in: V. Balzani, S. Campagna (Eds.), Photochemistry and Photophysics of Coordination Compounds I, Springer, Berlin/Heidelberg, 2007, pp. 69–115.
[12] C.T. Cunningham, K.L.H. Cunningham, J.F. Michalec, D.R. McMillin, Inorg. Chem. 38 (1999) 4388.
[13] D.G. Cuttell, S.M. Kuang, P.E. Fanwick, D.R. McMillin, R.A. Walton, J. Am. Chem. Soc. 124 (2002) 6.
[14] P.C. Ford, E. Cariati, J. Bourassa, Chem. Rev. 99 (1999) 3625.
[15] S. Perruchas, C. Tard, X.F. Le Goff, A. Fargues, A. Garcia, S. Kahlal, J.-Y. Saillard, T. Gacoin, J.-P. Boilot, Inorg. Chem. 50 (2011) 10682.
[16] D. Volz, D.M. Zink, T. Bocksrocker, J. Friedrichs, M. Nieger, T. Baumann, U. Lemmer, S. Bräse, Chem. Mater. 25 (2013) 3414.
[17] D.M. Zink, M. Baechle, T. Baumann, M. Nieger, M. Kuehn, C. Wang, W. Klopper, U. Monkowius, T. Hofbeck, H. Yersin, S. Braese, Inorg. Chem. 52 (2013) 2292.
[18] G.M. Sheldrick, SHELXS-97 (Program for Crystal Structure Solution), in, University of Götingen, Göttingen, 1997.
[19] G.M. Sheldrick, SHELXL-97 (Program for Crystal Structure Refinement), in, University of Götingen, Göttingen, 1997.
[20] G.W.T. M.J. Frisch, H.B. Schlegel, G.E. Scuseria, M.A. Robb, J.R. Cheeseman, G. Scalmani, V. Barone, B. Mennucci, G.A. Petersson, H. Nakatsuji, M. Caricato, X. Li, H.P. Hratchian, A.F. Izmaylov, J. Bloino, G. Zheng, J.L. Sonnenberg, M. Hada, M. Ehara, K. Toyota, R. Fukuda, J. Hasegawa, M. Ishida, T. Nakajima, Y. Honda, O. Kitao, H. Nakai, T. Vreven, J.A. Jr. Montgomery, J.E. Peralta, F. Ogliaro, M. Bearpark, J.J. Heyd, E. Brothers, K.N. Kudin, V.N. Staroverov, R. Kobayashi, J. Normand, K. Raghavachari, A. Rendell, J.C. Burant, S.S. Iyengar, J. Tomasi, M. Cossi, N. Rega, J.M. Millam, M. Klene, J.E. Knox, J.B. Cross, V. Bakken, C. Adamo,

J. Jaramillo, R. Gomperts, R.E. Stratmann, O. Yazyev, A.J. Austin, R. Cammi, C. Pomelli, J.W. Ochterski, R.L. Martin, K. Morokuma, V.G. Zakrzewski, G.A. Voth, P. Salvador, J.J. Dannenberg, S. Dapprich, A.D. Daniels, O. Farkas, J.B. Foresman, J.V. Ortiz, J. Cioslowski, D.J. Fox, C.T. Wallingford, Gaussian 09, in, Gaussian Inc, 2009.
[21] C.W. Hsu, C.C. Lin, M.W. Chung, Y. Chi, G.H. Lee, P.T. Chou, C.H. Chang, P.Y. Chen, J. Am. Chem. Soc. 133 (2011) 12085.
[22] F. De Angelis, S. Fantacci, A. Sgamellotti, E. Cariati, R. Ugo, P.C. Ford, Inorg. Chem. 45 (2006) 10576.
[23] L.-Q. Fan, Y.-Z. Huang, L.-M. Wu, L. Chen, J.-Q. Li, E. Ma, J. Solid State Chem. 179 (2006) 2361.
[24] É. Fournier, F. Lebrun, M. Drouin, A. Decken, P.D. Harvey, Inorg. Chem. 43 (2004) 3127.
[25] J.K. Bera, M. Nethaji, A.G. Samuelson, Inorg. Chem. 38 (1998) 218.
[26] K.-B. Shiu, S.-A. Liu, G.-H. Lee, Inorg. Chem. 49 (2010) 9902.
[27] Y.-Q. Song, Q.-Y. Lv, S.-Z. Zhan, J.-G. Wang, J.-Y. Su, A. Ding, Inorg. Chem. Commun. 11 (2008) 672.
[28] I.D. Salter, S.A. Williams, T. Adatia, Polyhedron 14 (1995) 2803.
[29] J.S. Field, R.J. Haines, B. Warwick, M.M. Zulu, Polyhedron 15 (1996) 3741.
[30] M. Trivedi, R. Nagarajan, A. Kumar, N.P. Rath, P. Valerga, Inorg. Chim. Acta 376 (2011) 549.
[31] W.-X. Chai, J. Lin, L. Song, L.-S. Qin, H.-S. Shi, J.-Y. Guo, K.-Y. Shu, Solid State Sci. 14 (2012) 1226.
[32] M.D. Halls, H.B. Schlegel, Chem. Mater. 13 (2001) 2632.
[33] Z.W. Liu, M.F. Qayyum, C. Wu, M.T. Whited, P.I. Djurovich, K.O. Hodgson, B. Hedman, E.I. Solomon, M.E. Thompson, J. Am. Chem. Soc. 133 (2011) 3700.
[34] L.L. Huo, W.X. Chai, L. Song, X.L. Zhang, Q.X. Tian, J.P. Liang, H.S. Shi, K.Y. Shu, Phosphorus Sulfur 188 (2013) 1340.
[35] D.B. Mitzi, K. Chondroudis, C.R. Kagan, Des. Inorg. Chem. 38 (1999) 6246.
[36] J. Roncali, Macromol. Rapid Commun. 28 (2007) 1761.